Chin. Geogra. Sci.
https://doi.org/10.1007/s11769-019-1066-7

Springer Science Press
www.springerlink.com/content/1002-0063

The 2012 Flash Drought Threatened US Midwest Agroecosystems

JIN Cui[1], LUO Xue[1], XIAO Xiangming[2, 3], DONG Jinwei[4], LI Xueming[1], YANG Jun[1], ZHAO Deyu[4]

(1. *College of Urban and Environment*, *Liaoning Normal University*, *Dalian* 116029, *China*; 2. *Department of Microbiology and Plant Biology*, *Center for Spatial Analysis*, *University of Oklahoma*, *Norman*, *OK* 73019, *USA*; 3. *Ministry of Education Key Laboratory of Biodiversity Science and Ecological Engineering*, *Institute of Biodiversity Science*, *Fudan University*, *Shanghai* 200433, *China*; 4. *Key Laboratory of Land Surface Pattern and Simulation*, *Institute of Geographic Sciences and Natural Resources Research*, *Chinese Academy of Sciences*, *Beijing* 100101, *China*)

Abstract: In the summer of 2012, the US Midwest, the most productive agricultural region in the world, experienced the most intense and widespread drought on record for the past hundred years. The 2012 drought, characterized as 'flash drought', developed in May with a rapid intensification afterwards, and peaked in mid-July. ~76% of crop region and 60% of grassland and pasture regions have been under moderate to severe dry conditions. This study used multiple lines of evidences, i.e., in-situ AmeriFlux measurements, spatial satellite observations, and scaled ecosystem modeling, to provide independent and complementary analysis on the impact of 2012 flash drought on the US Midwest vegetation greenness and photosynthesis carbon uptake. Three datasets consistently showed that 1) phenological activities of all biomes advanced 1–2 weeks earlier in 2012 compared to the other years of 2010–2014; 2) the drought had a more severe impact on agroecosystems (crop and grassland) than on forests; 3) the growth of crop and grassland was suppressed from June with significant reduction of vegetation index, sun-induced fluorescence (SIF) and gross primary production (GPP), and did not recover until the end of growing season. The modeling results showed that regional total GPP in 2012 was the lowest (1.76 Pg C/yr) during 2010–2014, and decreased by 63 Tg C compared with the other-year mean. Agroecosystems, accounting for 84% of regional GPP assimilation, were the most impacted by 2012 drought with total GPP reduction of 9%, 7%, 6%, and 29% for maize, soybean, cropland, and grassland, respectively. The frequency and severity of droughts have been predicted to increase in future. The results imply the importance to investigate the influences of flash droughts on vegetation productivity and terrestrial carbon cycling.

Keywords: food security; terrestrial carbon cycling; eddy covariance; Vegetation Photosynthesis Model; sun-induced fluorescence (SIF)

Citation: JIN Cui, LUO Xue, XIAO Xiangming, DONG Jinwei, LI Xueming, YANG Jun, ZHAO Deyu. The 2012 Flash Drought Threatened US Midwest Agroecosystems. *Chinese Geographical Science*. https://doi.org/10.1007/s11769-019-1066-7

1 Introduction

Droughts as an intermittent climate disturbance play an important role in the earth systems, and are predicted to increase under global warming conditions (Breshears et al., 2005; Dai, 2011; 2013). The drought impacts on the structure, composition, and function of terrestrial ecosystems are often diverse and difficult to determine (van der Molen et al., 2011; Reyer et al., 2013; Frank et al., 2015). These associated impacts are not only immediate, for example via directly affecting plant photosynthesis and respiration (Ciais et al., 2005), but can exhibit time-lagged effects, such as increasing pest and pathogen-caused vegetation mortality, and changing plant species composition (Bigler et al., 2007; Phillips et al., 2010).

Received date: 2018-10-10; accepted date: 2019-02-03
Foundation item: Under the auspices of the National Natural Science Foundation of China (No. 41801340), Natural Science Foundation of Liaoning, China (No. 20180550238), the Key Research Program of Frontier Sciences by Chinese Academy of Sciences (No. QYZDB-SSW-DQC005)
Corresponding author: ZHAO Deyu. E-mail: zhaody@igsnrr.ac.cn

Recently, 'flash drought' has started to be widely used to refer to the short-term drought events with a rapid onset and intensification rate (Svoboda et al., 2002). Unlike those droughts that develop slowly, most climate models failed to early predict flash droughts (Hoerling et al., 2014). Moreover, flash droughts are likely to occur during vegetation growing seasons—the sensitive stages of crop development, and allow less time for agricultural community to adapt to the changing conditions (Otkin et al., 2013). Thus, flash droughts are extremely devastating to agriculture. Numerous studies have examined the impacts of droughts on vegetation greenness and productivity, and terrestrial carbon budgets on the regional to subcontinental scales (Ciais et al., 2005; Zhao and Running, 2010; Schwalm et al., 2012; Zhang et al., 2012; Liu et al., 2014). These studies, however, focused on the slowly developed droughts, and the influences of flash droughts on ecosystems have been less investigated (Mo and Lettenmaier, 2016; Otkin et al., 2016; 2018).

In general, three approaches are applied to study the ecosystem response to droughts: in-situ eddy covariance sites (Dunn et al., 2007; Granier et al., 2007; Noormets et al., 2010; Wolf et al., 2013), spatial satellite observations (Ji and Peters, 2003; Vicente-Serrano, 2007; Asner and Alencar, 2010), and ecosystem modeling (Zhao and Running, 2010; Liu et al., 2014; Williams et al., 2014; Zscheischler et al., 2014). All these approaches, however, have limitations. Although the eddy covariance observations can provide a relatively precise understanding on the stand-scale functional response of vegetation to droughts, the number of sites is limited spatially when assessing the ecosystem-scale impact. While remote sensing and ecosystem modeling are the best suitable to investigate large-scale drought effects, remote sensing can only show a view via the spectral reflectance changes expressed as vegetation indices instead of direct indicators of vegetation leaf area, biomass and physiological functioning, and some ecosystem models are difficult to accurately capture the response of vegetation physiological process to environmental stressors due to model structure and temporal resolution. Hence, an integrated analysis of in-situ observations, remote sensing, and ecosystem modeling can overcome shortcomings of each approach, and is indispensable to comprehensively reveal the cross-scale response of ecosystem to drought (Reichstein et al., 2007; Reyer et al., 2013).

The US Midwest is one of the most intense areas of agriculture in the world. However, due to extremely cold, dry air masses from northern Canada and Alaska and warm, humid air masses from the Gulf of Mexico, the region is under a wide range of climate extremes, such as droughts and floods. Projections from climate models indicate an increase in the chance of droughts over the US Midwest in future (Naumann et al., 2018). Crop systems become more sensitive and vulnerable to summer temperature extremes (Lobell et al., 2014; Mueller et al., 2016; Jin et al., 2018). In 2012, the US Midwest experienced severe flash drought during the summertime. The extreme drought condition destroyed the major field crops, particularly field corn and soybeans, and caused large loss in livestock producers due to forage and feed decreasing (Boyer et al., 2013; Mallya et al., 2013). The objectives of this study are to 1) evaluate the timing, severity, and spatial extent of 2012 flash drought over the US Midwest, and 2) investigate the impact of 2012 flash drought on the US Midwest ecosystems with a joint analysis of ground observations, remote sensing, and ecosystem modeling.

2 Materials and Methods

2.1 In-situ AmeriFlux data

The AmeriFlux is an extensive network of eddy covariance flux sites measuring ecosystem-scale CO_2, water,

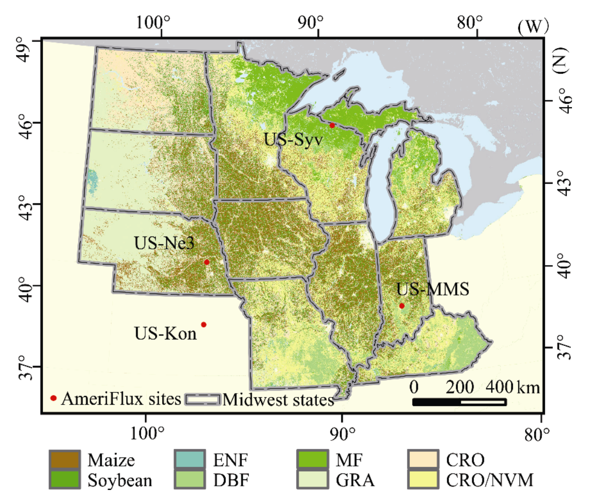

Fig. 1 Land use and land cover map of the US Midwest in 2014. The AmeriFlux sites are indicated by the red circles. Vegetation type is coded according to IGBP designations: ENF, evergreen needle forest; DBF, deciduous broadleaf forest; MF, mixed forest; GRA, grassland; CRO, cropland; CRO/NVM, cropland/natural vegetation mosaic

and energy fluxes over North America. This study collected four sites with homogenous footprint. As no grassland site was located in the US Midwest, we used one nearby site in the Konza Prairie, Kansas (US-Kon) as a proxy. We obtained the gap-filled Level-2 product of climate variables, soil water content (SWC), and CO_2 fluxes of four different-biome sites during 2010–2014 (http://ameriflux.ornl.gov/) (Fig.1, Table 1), then aggregated the Level-2 data to 8-day intervals to match with satellite observations.

2.2 Regional data for the 2012 flash drought assessment

We used high-quality spatial climate data from the PRISM (Parameter-evaluation Regressions on Independent Slopes Model) climate mapping program to delineate 2012 anomalous climate. The PRISM provides a set of fine-scale daily to annual climate variables from 1895–present, primarily for the Conterminous United States (Daly et al., 2000). The daily 4 km mean air temperature and precipitation of PRISM during 2010–2014 were required from the PRISM climate group at http://www.prism.oregonstate.edu/. The Standardized Precipitation Index (SPI) was also acquired to quantify the drought intensity during 2012 growing season (from April to September). The SPI measures the probability of observed precipitation based on historical records at a variety of time scales for both short- and long-term droughts (McKee et al., 1993). As this study focused on the short-term agricultural applications, the 1-month SPI from the National Drought Mitigation Center was obtained at the Western Regional Climate Center (http://www.wrcc.dri.edu/spi/spi.html). A drought event occurs when the SPI reaches an intensity of –0.5 or less. Value ranges of –0.5 to –0.8, –0.8 to –1.3, –1.3 to –1.6, –1.6 to –2.0, defined by National Climatic Data Center (NCDC), stand for abnormal, moderate, severe, and extreme drought, respectively.

2.3 Regional data for regional GPP estimation

2.3.1 NCEP/NARR climate data

The North American Regional Reanalysis (NARR) by the National Centers for Environmental Prediction (NCEP) is a long-term regional reanalysis of the near-surface meteorological variables over North America (Mesinger et al., 2006). The NARR is produced at a spatial resolution of 32 km and a temporal resolution of 3-hour. We obtained the NARR 3-hourly air temperature and downward shortwave radiation from http://www.esrl.noaa.gov/psd/. The 3-hourly NARR was aggregated to 8-day intervals, then was spatially interpolated to a spatial resolution of 500 m. As the NARR downward shortwave radiation was further calibrated due to systematically positive bias. See Zhang et al. (2016) and Jin et al. (2015) for detailed interpolation and calibration algorithms, respectively.

2.3.2 MODIS surface reflectance and vegetation indices

Three vegetation indices, the Normalized Difference Vegetation Index (NDVI), Enhanced Vegetation Index (EVI), and Land Surface Water Index (LSWI), were calculated as followings：

$$NDVI = \frac{\rho_{\mathrm{NIR}_1} - \rho_{\mathrm{red}}}{\rho_{\mathrm{NIR}_1} + \rho_{\mathrm{red}}} \tag{1}$$

$$EVI = \frac{\rho_{\mathrm{NIR1}} - \rho_{\mathrm{red}}}{\rho_{\mathrm{NIR}_1} + 6 \times \rho_{\mathrm{red}} - 7.5 \times \rho_{\mathrm{blue}} + 1} \tag{2}$$

$$LSWI = \frac{\rho_{\mathrm{NIR}_1} - \rho_{\mathrm{SWIR}_1}}{\rho_{\mathrm{NIR}_1} + \rho_{\mathrm{SWIR}_1}} \tag{3}$$

where ρ_{NIR_1}, ρ_{red}, ρ_{blue} and ρ_{SWIR_1} are the MOD09A1 surface reflectance for NIR_1 (841–876 nm), red (620–670 nm), blue (459–479 nm), and SWIR_1 (1628– 1652 nm), respectively.

2.3.3 NASS Cropland Data Layer

The Cropland Data Layers (CDLs) provided by the US Department of Agriculture (USDA) National Agricultural Statistics Service (NASS) are the satellite-based crop-specific land cover datasets at a fine spatial resolution of 30 m or 56 m. The classification accuracy accuracies for maize and soybean on the CDLs are above 90 % (Boryan et al., 2011). The annual CDLs of 2010–2014 were aggregated to 500-m spatial datasets of areal fraction for maize and soybean.

2.3.4 MODIS land cover product

The MODIS Land Cover Type product (MCD12Q1) describes land cover properties derived from annual satellite observations on Terra- and Aqua-MODIS. MCD12Q1 was used as the base map to assign biome parameters when estimating GPP for non-maize/soybean crops and non-crop biomes, including pasture/grassland, mixed forest (MF), deciduous broadleaf forest (DBF).

2.4 Other regional datasets

2.4.1 GOME-2 sun-induced fluorescence (SIF)

SIF is derived from the spectral radiance at 740 nm measured by the Global Ozone Monitoring Experiment 2 (GOME-2) onboard the MetOp-A platform. GOME-2 SIF has shown the potential of a direct measurement of GPP for crop and grassland on both in-situ and regional levels (Guanter et al., 2014; Zhang et al., 2014). We used the weekly and monthly Level-2 GOME-2 SIF (version 2.6) as an indicator of the Midwest-wide ecosystem production. Detailed description about the GOME-2 SIF retrievals can be found via Joiner et al. (2013).

2.4.2 USDA NASS agricultural inventory data (Yield$_{NASS}$)

State-level yield statistics of maize, soybean, and pasture/grassland were acquired from the USDA NASS Quick Stats database (http://quickstats.nass.usda.gov/).

2.5 Regional Gross Primary Production (GPP) estimation

The Vegetation Photosynthesis Model (VPM) simulates the terrestrial ecosystem GPP based on the concept of the light absorption by canopy chlorophyll (Xiao et al., 2004a, b):

$$GPP = \varepsilon \times fPAR_{\mathrm{chl}} \times PAR \tag{4}$$

$$\varepsilon = \varepsilon_0 \times T_{\mathrm{salar}} \times W_{\mathrm{scalar}} \tag{5}$$

where PAR is the photosynthetically active radiation; $fPAR_{chl}$ is the fraction of PAR absorbed by canopy chlorophyll. ε is the light use efficiency, a function of the maximum light use efficiency (temperature and water condition status: T_{scalar}, W_{scalar}). The VPM parameters were derived from the satellite ($fPAR_{\mathrm{chl}}$, W_{scalar}) and weather reanalysis (PAR, T_{scalar}) data in above section, see Xiao et al. (2004a), Xiao et al. (2004b) for parameter calculation.

The NASS CDLs allowed us to separate GPP contributions of maize and soybean within each 500 m pixel. To consider the photosynthesis capacity difference between maize (C4) and soybean (C3), we applied in-situ derived ε_0 of 3.12 g C/MJ and 1.75 g C/MJ for maize and soybean, respectively. A biome parameter lookup table containing values of ε_0 and biome-specific physiological parameters for other vegetation types was referred to Zhang et al. (2016). The GPP of one pixel was estimated by area-weighted averaging contributions of sub-pixel components based on the area fraction maps of maize and soybean, and MCD12Q1 land cover datasets:

$$GPP_{\mathrm{VPM}} = \sum\nolimits_i f_i \times \varepsilon_{0i} \times fPAPR_{\mathrm{chl}} \times PAR \tag{6}$$

where f_i and ε_{0i} are the area fraction and light use efficiency for maize, soybean, other vegetation type (crop, grassland, DBF, MF, *etc.*), respectively. We simulated GPP over the US Midwest from 2010 to 2014. The GPP datasets have been validated via estimated GPP from in-situ AmeriFlux sites (Fig. S1), biweekly SIF for each biome (Fig. S2), and linear regression analysis between SIF and GPP_{VPM} on 0.5° grid cell (Fig. S3).

2.6 Data analysis

We compared the 2012 monthly air temperature and precipitation with the mean conditions of 2010–2014 to track the onset and persistence of 2012 drought over the US Midwest agroecosystem region. We also calculated the mean and minimum of 1-month SPI and the anomalies of temperature and precipitation to quantify the spatial extent and severity of 2012 flash drought during growing season.

The drought impact on ecosystems were first evaluated at four AmeriFlux in-situ sites by analyzing the differences in climates, soil water, phenology, CO_2 fluxes during the 2012 growing season relative to long-term means. As long-term observations are usually not available for AmeriFlux sites, we used the mean of 2010–2014 (excluding 2012) or single year (if multiple years were unavailable) as a proxy of 'normal' condition.

Multiple time series datasets, including the satellite-derived vegetation greenness (NDVI, EVI, LSWI), satellite-measured ecosystem production (SIF), terrestrial carbon cycle modelling (GPP_{VPM}), and agricultural inventory ($\mathrm{Yield}_{\mathrm{NASS}}$), were applied to investigate the Midwest-wide ecosystem changes. We quantified change magnitudes and response dates of vegetation greenness and productivity during the 2012 flash drought compared to 2010–2014 at biome and pixel levels.

3 Results

3.1 Assessment of 2012 flash drought

The sign of 2012 flash drought can be traced back to unusually warm winter and spring (i.e., January through April) (Fig. 2). The spring of 2012 was the warmest spring on record in the US Midwest. Air temperature averaged over the US Midwest was 4℃ (February) and 9℃ (March) higher than the 2010–2014 means. The drought rapidly developed in late spring/early summer (May). Drought severity abruptly intensified and continued to increase because of the significant precipitation deficit and heat wave. The drought peaked in June and July with the precipitation decreasing by 62% and 54% and temperature increasing by 1.5℃ and 3℃ relative to the 2010–2014 means, respectively. From September 2012, drought severity began to ameliorate due to near-normal precipitation. Overall, the averaged accumulated precipitation of 2012 growing season over the US Midwest was 235 mm, which was 46% below the 2010–2014 mean.

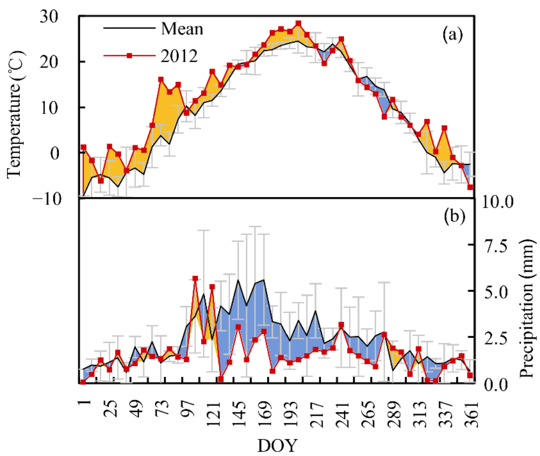

Fig. 2 Time series of 8-day averaged air temperature (a) and precipitation (b) from PRISM over the US Midwest. The red line with markers represents 2012; black lines denote the 2010–2014 mean (excluding 2012); vertical bars indicate mean ± standard deviation; shading areas represent 2012 anomalies relative to other-year means of 2010–2014 (brown shows 2012 > mean, blue 2012 < mean)

The severity of 2012 flash drought during growing season spatially varied across the US Midwest (Fig. 3). Most of the region was under abnormally dry to extreme droughts with the concurrence of high temperature and marked water deficit (Figs. 3d–3e) except the upper Great Lakes region and eastern states under normal moist conditions (Fig. 3a). The south region (~46% of the US Midwest), including large extents of South Dakota, Nebraska, Iowa, Missouri, Illinois, Indiana, and Kentucky, has experienced extreme drought in June or July (Figs. 3b–3c). In particular, 76% of maize/soybean region suffered from moderate to extreme drought with 1.2℃ of temperature increase and –221 mm of precipitation deficit. 59% of grassland/pasture region was under extreme drought with the temperature and precipitation anomalies of 1.8℃ and –267 mm, respectively.

3.2 Impacts of 2012 flash drought on the US Midwest ecosystems at in-situ sites

We compared climate conditions, soil moisture, vegetation growth (phenology and CO_2 fluxes) between 2012 and normal condition (2010–2014 mean) at AmeriFlux sites (Fig. 4 and Table 1). Climate changes of 2012 from instrumental observations were consistent with the PRISM drought assessment in Section 3.1. All sites experienced warm temperature ($\Delta T > 0$) and water deficit (ΔP, $\Delta SWC < 0$) during the 2012 growing season. Particularly, SWC was greatly lower than 2010–2014 means for soybean (–38%) and grassland (–31%) sites.

Four sites showed a uniform phenological response to 2012 extreme climate. SOS, MAXT, and EOS in 2012 were 1 or 2 weeks earlier compared to 2010–2014 means. Soybean and grassland were significantly affected, showing that GPP, NEE, and R_{eco} decreased significantly ($P < 0.001$, $n = 10$) in parallel with soil water reduction in early July and June, respectively, and didn't recover afterwards (Fig. 4a–4b). A large reduction of

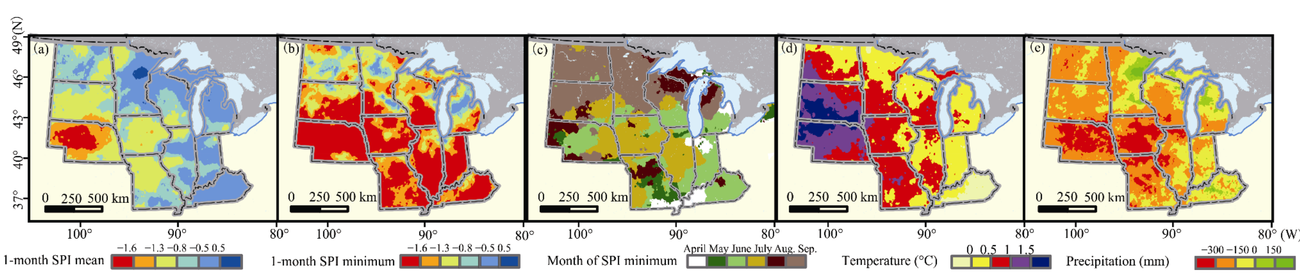

Fig. 3 Spatial pattern of drought severity and climate anomalies during 2012 growing season (May–September) over the US Midwest. (a)–(b) 1-month SPI mean and minimum. (c) month of SPI minimum. (d)–(e) anomalies of air temperature and total precipitation of 2012 growing season relative to other-year means of 2010–2014

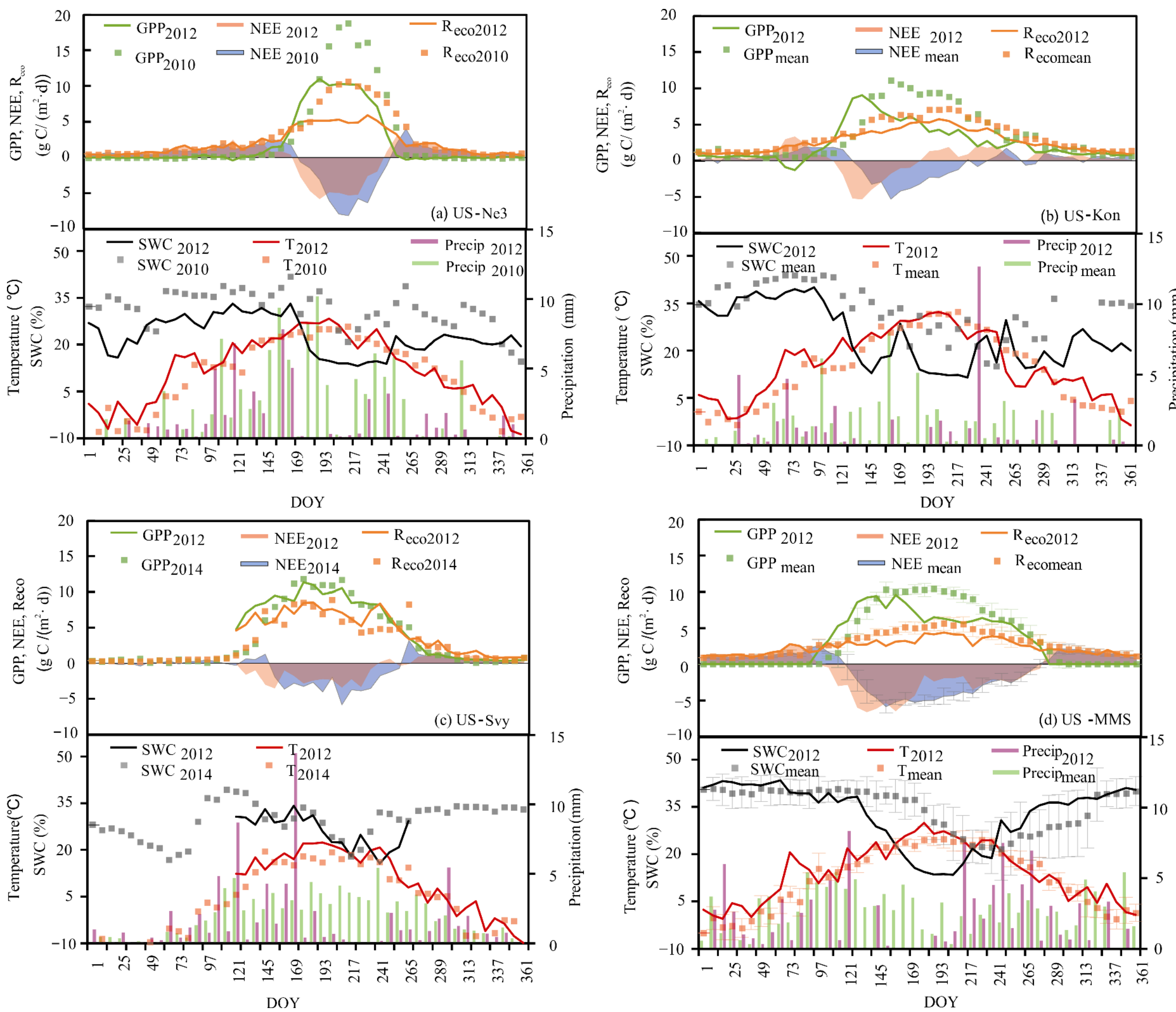

Fig. 4 Observed climate, soil water content, and CO_2 fluxes at four AmeriFlux sites. GPP: 8-day averaged gross primary production; NEE: 8-day averaged Net ecosystem exchange; R_{eco}: 8-day Ecosystem respiration ; T: 8-day averaged air temperature at 2 m; SWC: Soil Water Content; Precip: 8-day accumulated precipitation; GPP_{mean}, NEE_{mean}, $R_{ecomean}$, T_{mean}, SWC_{mean}, and $Precip_{mean}$ are the means of GPP, NEE, R, T, SWC, and Precip during 2010–2014, respectively. DOY: day of year

Table 1 Changes in climate, soil moisture, vegetation phenology, and seasonal CO_2 fluxes between 2012 and 2010–2014 mean at four AmeriFlux sites during growing season

Site Code	Name	Biome	Lat, Lon	Years	SOS		MAXT		EOS		Growing season					
					2012	mean	2012	mean	2012	mean	ΔT	ΔP	ΔSWC	ΔGPP	ΔNEE	ΔR_{eco}
US-Ne3	Mead Rainfed	CRO	41.18, –96.44	2010, 2012	06/02	06/10	07/12	07/28	09/06	09/14	1.5	–3.0	–11	–324	–21	–302
US-Kon	Konza Prairie	GRA	39.08, –96.56	2010–2012	04/07	04/15	05/17	06/10	11/01	11/17	0.5	–1.0	–9	–357	–141	–216
US-Syv	Sylvania Wilderness	MF	46.24, –89.35	2012, 2014	–	–	07/04	07/04	10/16	10/24	2.5	–1.0*	–4	75	–27	103
US-MMS	Morgan Monroe State Forest	DBF	39.32,–86.41	2010–2014	04/07	04/23	05/25	06/02	10/08	10/16	0.3	–0.5	–5	–169	25	–174

Notes: Lat-latitude; Lon-Longitude (°); SOS-start of season (leaf-on date when GPP ≥ 1 g C/(m^2·d)); MAXT-time of maximum photosynthesis; EOS-end of season (leaf-off date when GPP ≥ 1 g C/(m^2·d)); ΔT, ΔP, ΔSWC, ΔGPP, ΔNEE, ΔR_{eco} stand for the difference of temperature (℃/d), precipitation (mm/d), soil water content (%/dy), total gross primary productivity, net ecosystem exchange, and ecosystem respiration (g C/m^2) between 2012 and 2010–2014 mean during growing season. *We used precipitation from US-PFa (78 km away) to replace the missing data at US-Syv in 2012 seasonal GPP was found at –324 g C/m^2 (–29.9%) for soybean and–357 g C/m^2 (–29.6%) for grassland relative to 2010–2014 means. In contrast, drought had less impact on carbon fluxes of forest sites. At US-Syv, dry spell of 2012 late August didn't cause the significant difference of ecosystem productivity from other-year mean (P = 0.31, n = 10) (Fig. 4c), and seasonal GPP of 2012 increased (~75 g C/m^2 above mean) due to warm spring. At US-MMS, GPP began to decrease from mid-June 2012, then recovered in mid-August (Fig. 4d).

3.3 Impacts of 2012 flash drought on the US Midwest ecosystems at regional scale

Fig. 5 shows intra-annual variations of five spatially averaged satellite-based vegetation biophysical parameters for different biomes in 2012 and 2010–2014 mean on 8-day intervals. For individual biome, we found good agreement among NDVI, EVI, LSWI, GPP_{VPM}, SIF when indicating its ecosystem response (i.e. response timing and changing magnitude) to 2012 drought. Shading areas in Fig. 5 showed that all biomes experienced advanced phenology in 2012 with a largest reduction of NDVI, EVI, LSWI, GPP_{VPM}, and SIF occurring in August. Consistent with in-situ observations in section 3.2, agricultural biomes (maize, soybean, overall crop and grassland) were more affected than forests. Maize emerged ~2 weeks (DOY = 137 when greenness and production started to increase) earlier than soybean (earlier June, DOY = 153). However, extreme heat and lack of precipitation suppressed maize, soybean, and crop growth after July. Compared to multi-year averages, vegetation indices, GPP_{VPM}, and SIF of pasture/grassland began to fail in ~ late-May (DOY = 145) with the largest growing-season reduction rate of 24% (NDVI), 22% (EVI), 217% (LSWI), 33% (GPP_{VPM}), and 22% (SIF). Slightly different from in-situ observations, NDVI, EVI, LSWI, GPP_{VPM}, and SIF showed subtle decrease for both MF (–9% to –2%) and DBF (–8% to –2%) after July on biome scale.

We quantified the Midwest-wide changing magnitudes of vegetation greenness and production during April–June (AMJ), July–September (JAS), and growing season (GS) of 2012, and also mapped vegetation response dates to 2012 drought on 500 m or 0.5° pixel level (Fig. 6). In AMJ, vegetation greenness, GPP_{VPM} and SIF over half of the US Midwest apparently increased (RCR > 0%), whereas the mixed prairie region, including southwestern North Dakota, main South Dakota, and western Nebraska, experienced the largest reduction (Fig. 6a). In JAS, the crop region was also suppressed by drought besides the west prairie. Over ~ 80% of the US Midwest showed declines (RCR < 0%) in NDVI (85%), EVI (87%), LSWI (87%), GPP_{VPM} (80%), and SIF (86%) except the forest regions in the upper northern Great Lakes, southeast Missouri, and Kentucky,

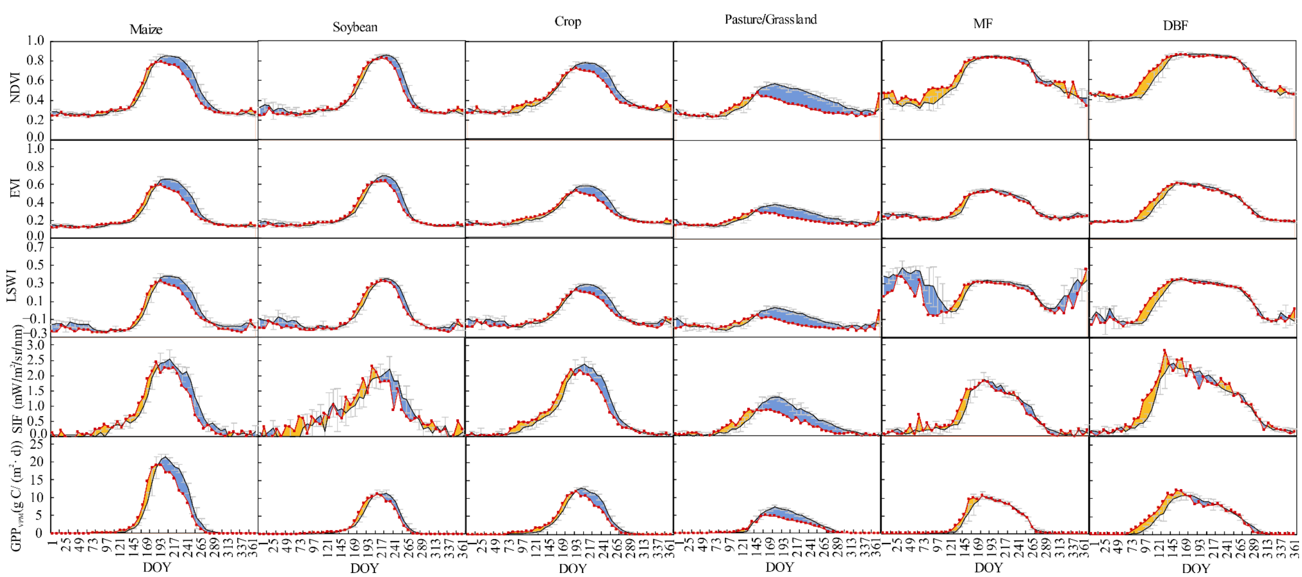

Fig. 5 Intra-annual variations of the spatially averaged 8-day vegetation greenness (NDVI, EVI, LSWI), SIF, and GPP_{VPM} for different biomes. DOY: day of year. Red lines with markers represent 2012; black lines denote the 2010–2014 mean (excluding 2012), and vertical bars indicate mean ± standard deviation; shading areas represent 2012 anomalies relative to other-year means of 2010–2014 (brown shows 2012 > mean, blue 2012 < mean)

and parts of agriculture regions in the Minnesota River basin, and James and Red River basins of North Dakota (Fig. 6b). Overall, the main agroecosystems of Midwest were the most negatively drought-affected during the 2012 growing season, covering North Dakota, South Dakota, Nebraska, Iowa, Missouri, Illinois, and Indiana (Fig. 6c). The reduction of vegetation greenness and productivity in these regions followed the drought pattern exhibited in Fig. 3. For example, Nebraska was continuously under severe to extreme drought conditions during 2012 growing season. At least one-month extreme drought has attacked these agricultural regions (Fig. 3b), and it occurred mainly in June or July (Fig. 3c).

Vegetation response timing to the 2012 flash drought also spatially varied across the US Midwest, and its spatial pattern was relatively consistent among five vegetation biophysical parameters (Fig. 6d). The prairie region responded earliest, and vegetation indices, GPP_{VPM}, and

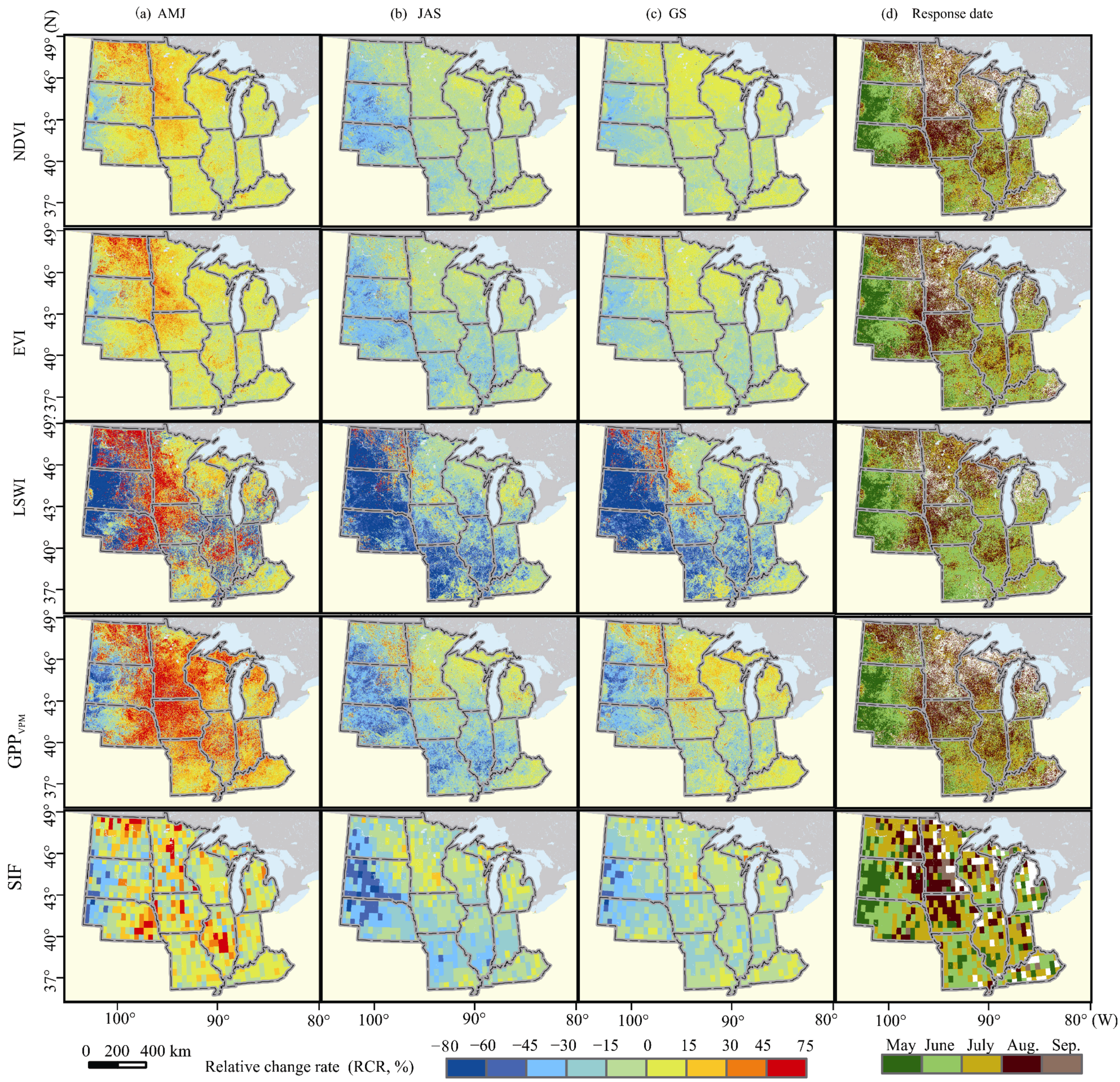

Fig. 6 Midwest-wide relative change rate (RCR, %) and response date of 8-day vegetation greenness (NDVI, EVI, LSWI), productivity (GPP_{VPM} and SIF) during the 2012 flash drought relative to the other-year means of 2010–2014. (a)–(c) RCR during April–June (AMJ), July–September (JAS), and growing season (GS). (e) response date to drought: the first date when there are three 8-day composites in 2012 were continuously below the other-year means of 2010–2014. The insets show the frequency histograms of RCR and response date

SIF started to drop below the multi-year averages in May and June. The major crop regions responded to drought mainly in August except that the crop suppression in northern Missouri occurred earlier (June and July). This finding agreed with USDA NASS Crop Progress Report when comparing Missouri with other states. The forests in upper Great Lakes and southeast Kentucky did not show obvious decline during the drought, whereas deciduous forest regions in the southern Missouri and Indiana decreased in July.

Regional total GPP in 2012 was the lowest (1.76 Pg C/yr) during the period of 2010–2014 (Table 2), and drought reduced total GPP by 63 Tg C/yr (3.5%) compared with the other-year mean of 2010–2014. Agroecosystems, accounting for 84 % of regional GPP assimilation, were the most impacted (negatively) by 2012 drought. Maize, soybean, cropland, and grassland exhibited the lowest annual/total GPP in 2012 with reductions of 9%, 7%, 6%, and 29% respectively for annual GPP and 3%, 10%, 4%, and 28% respectively for total GPP. Grassland showed rapid recovery of carbon assimilation following drought, and annual GPP in 2013 for grassland reached back to annual GPP in 2010 (0.69 kg C/(m^2·yr)). Annual GPP of maize, soybean and crop gradually increased during 2013–2014, however, was lower than the values in 2010. In opposite to agroecosystems, annual/total GPP in 2012 for forests increased in relative to the other-year means of 2010–2014. As the 2012 flash drought induced lagged negative impact on of forests, annual GPP of MF and DBF reached the lowest in 2013 and 2014, respectively.

Agricultural harvest data can also indicate the influences of 2012 flash drought on agroecosystem productivity and carbon cycles. Agricultural harvest data reported negative anomalies of $\text{Yield}_{\text{NASS}}$ for maize and soybean in 2012 over most Midwest states except North Dakota (ND) and Minnesota (MN). This result was consistent with ecosystem modeling (GPP_{VPM}) (Figs. 7a–7b, 6c). Both $\text{Yield}_{\text{NASS}}$ and GPP_{VPM} of pasture/grassland declined over three main growing states (Fig. 7c).

Table 2 Annual and total GPP estimates for each biome of the US Midwest from 2010 to 2014

Biome		2010	2011	2012	2013	2014	2012 AC	2012 RC
Maize	Area	232644	249535	263390	257493	243753		
	Annual GPP	1.61	1.55	1.42	1.53	1.58	–0.15	–9
	Total GPP	0.37	0.39	0.37	0.39	0.39	–11	–3
Soybean	Area	192304	191286	188958	193132	214248		
	Annual GPP	0.91	0.88	0.83	0.87	0.90	–0.06	–7
	Total GPP	0.17	0.17	0.16	0.17	0.19	–18	–10
Maize and soybean	Total GPP	0.55	0.55	0.53	0.56	0.58	–29	–5
CRO	Area	779765	769556	786575	769695	769696		
	Annual GPP	1.11	1.07	1.03	1.07	1.09	–0.06	–6
	Total GPP	0.86	0.82	0.81	0.83	0.84	–31	–4
GRA	Area	265315	264856	275767	281087	281085		
	Annual GPP	0.69	0.68	0.49	0.69	0.70	–0.20	–29
	Total GPP	0.18	0.18	0.14	0.19	0.20	–52	–28
CRO/NVM	Area	420092	418490	384771	403613	403613		
	Annual GPP	1.27	1.23	1.27	1.21	1.22	0.04	3
	Total GPP	0.53	0.51	0.49	0.49	0.49	–18	–4
MF	Area	127428	141064	143788	139160	139160		
	Annual GPP	0.97	1.01	1.05	0.92	1.00	0.08	8
	Total GPP	0.12	0.14	0.15	0.13	0.14	18	14
DBF	Area	112175	106294	113332	109645	109652		
	Annual GPP	1.44	1.41	1.53	1.39	1.37	0.13	9
	Total GPP	0.03	0.03	0.04	0.03	0.03	4	13
All biomes	Total GPP	1.87	1.81	1.76	1.79	1.82	–63	–4

Notes: area (km^2), area over 500 m pixels, for maize and soybean, pixels with area fraction over 20%; annual GPP (kg C/(m^2 ·yr)), spatially averaged annual GPP; total GPP (Pg C/yr), spatially integrate annual GPP; 2012 AC (Tg C/yr), actual change of total GPP in 2012 relative to the other-year mean of 2010–2014; 2012 RC (%), relative change rate of total GPP in 2012 relative to the other-year mean of 2010–2014

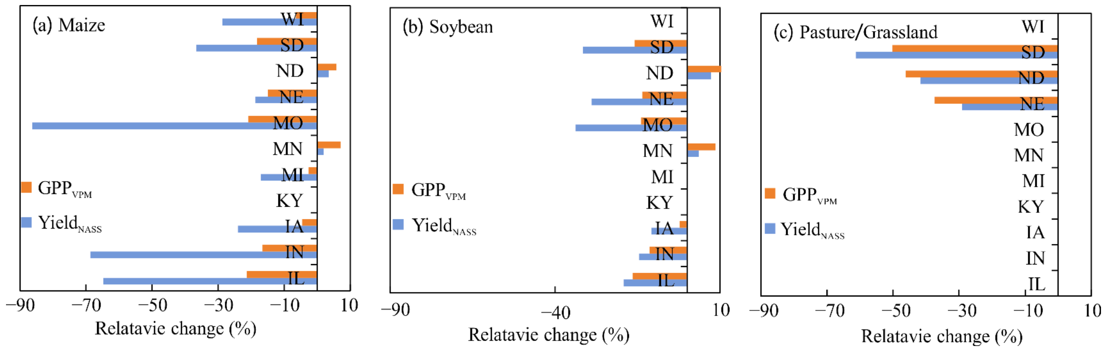

Fig. 7 Relative change (%) of GPP_{VPM} and NASS yield statistics ($Yield_{NASS}$) over the US Midwest states for maize (a), soybean (b), and pasture/grassland (c). To avoid statistic errors in regions with sparse agriculture cultivation, analysis are limited to states where maize, soybean, or pasture/grassland account for > 20% of the total state area

4 Discussion

4.1 Flash Droughts in the US Midwest

The 2012 flash drought in the US Midwest is the one of the worsts during the past years on record with comparable severity and spatial extent of those in 1930s, 1950s, and 1980s (Hoerling et al., 2014; Kellner and Niyogi, 2014). The 2012 flash drought mostly attacked the entire Midwest, and it was not captured by the US Drought Monitoring until late June due to its rapid onset in May. Mallya et al. (2013) concluded that the weak winter storms in previous winter triggered by anomalous tropical see surface temperatures (SSTs), La Niña, was the main causes of 2012 drought. Two recent studies, however, showed that the 2012 flash drought more likely related to natural weather variations causing the reduction of cyclone and frontal activity in late spring, and the decrease of moisture transportation from Gulf of Mexico instead of SST anomalies (Kumar et al., 2013; Hoerling et al., 2014). According to the multi-model projections, the probability of severe droughts and heat waves was predicted to increase over the continental United States in future (Wehner et al., 2011; Basara et al., 2013; Wuebbles et al., 2014; Cook et al., 2015). Hence, heat and drought extremes will continue to significantly affect the terrestrial ecosystem, such as by changing the exchange of carbon fluxes between land and atmosphere.

4.2 Impacts of 2012 flash drought on the US Midwest ecosystems

This study, using multiple lines of evidences, showed that the 2012 flash drought significantly affected on the US Midwest ecosystems by changing vegetation function, structure, and phenology. Similar to slowly-developed or prolonged drought, flash drought causes direct effects on ecosystem function by modifying carbon assimilation (GPP) and release. The high temperature and water-limited conditions during droughts lead to stomatal closure, membrane damage, and disturbing activities of photosynthesis enzymes, therefore, CO_2 diffusion to leaf and photosynthetic capacity are reduced accordingly (Reddy et al., 2004; Farooq et al., 2009). Drought can also trigger changes in vegetation structure, such as the decrease of green leaf area due to leaf angle change within canopy and leaf senescence, and shorten growing season length, thus indirectly cause further decline in carbon assimilation (van der Molen et al., 2011). During the 2012 flash drought, the in-situ observations, vegetation indices, and ecosystem modeling results showed the relative consistency in changing trends of vegetation phenology, greenness, and productivity across stand, biome, and regional levels. In 2012 spring, warm weather and close-to-normal precipitation triggered the growth of natural vegetation and encouraged the farmers' planting activities resulting to the planting and emergence dates for agricultural crops shifting earlier. In 2012 summer, on the other hand, high temperature and soil water deficit inhibited plant photosynthesis and caused leaf senescence earlier, and leaded to lower productivity. Even though the warm spring with higher vegetation greenness and productivity offset the impact of summer drought in 2012, the drought still caused significant negative effects on vegetation greenness and productivity for the whole year over the US Midwest.

The vegetation greenness and productivity among ecosystem and land cover types reacted differently to the 2012 flash drought. Grassland and prairie regions rapidly responded on the drought started to develop in May, and exhibited the largest declines in greenness and productivity during the growing season. The productivity reduction of crops mainly began from July, when the growth stages (grain and pod filling) of maize and soybean were the most sensitive to water stress. On the other hand, significant negative impacts of drought on forests were not found in this study. One reason is that the deep rooting systems alleviate water stress in many forests. Other factors, such as drought severity, timing of drought, drought-associated higher incident radiation, and dominant species, should also be accounted. In this study, forests only experienced less severe dry condition than agricultural region did in 2012. Overall, the agroecosystems of the US Midwest were more vulnerable to the 2012 flash drought than forests.

4.3 Challenges in terrestrial ecosystem models for agroecosystems

Numerous studies have estimated ecosystem productivity at regional or larger scales, and projected its changes in response to climate change and climate variability using either semiempirical diagnostic models or process-based biogeochemistry models (Ciais et al., 2005; Reichstein et al., 2007; Sitch et al., 2008; Zhao and Running, 2010; Zhang et al., 2016). However, a large range of uncertainties related to cropland were often ignored in these models (Schwalm et al., 2010; van der Molen et al., 2011; Chen et al., 2014). One main reason is that these models fail to consider the growth modules for specific crops, such as C4 crops. For example, it has been widely verified that MODIS standard GPP product (MOD17) assigns a universal ε_0 (1.04 gC/MJ) for all crop species with different photosynthetic pathway (C3 and C4), and resulted to large underestimate of GPP for C4 crops (Zhang et al., 2008; Chen et al., 2014; Xin et al., 2015). An intercomparison of 26 terrestrial ecosystem models in part by the North American Carbon Project (NACP) found that all models performed poorly when estimating the GPP for crop and grassland (Schaefer et al., 2012). Recently, Guanter et al. (2014) inferred that the crop GPP derived from GOME-2 SIF were 50%–75% higher than GPP estimates from state-of-art carbon models over US Corn Belt, including ten process-based DGVMs (Dynamic Global Vegetation Models), MPI-BGC (Max Planck Institute for Biogeochemistry) model, and MOD17. To accurately simulate regional GPP, this study used annual fine-resolution crop type maps from the NASS CDL f to improve the parameterization of ε_0 in the VPM model for maize (C4) and soybean (C3), and took account of the sub-pixel variability for C3 and C4 photosynthetic pathways within each 500 m pixel. The results indicated the great potential of VPM to simulated the observed eddy-covariance GPP for maize, soybean, MF, DBF on in-situ sites (Fig. S1). In the meanwhile, the capacity to model GPP on individual biome and regional scales was further verified via GOME-2 SIF in 2010−2014 (see supplementary Figs. S2–S3). We further compared GPP estimates from three diagnostic models (VPM, MOD17, and MPI-BGC), four Trendy DGVMs with GOME-2 SIF in July 2010 over the US (Fig. 8). Similar to the global analyses of Zeng et al. (2014) of Guanter et al. (2014), the US Corn Belt, the intensively cultivated and highly productive region, had remarkably highest SIF signals in July. Only the VPM and VEGAS captured this SIF pattern over the US Corn Belt, not by the other five models. In addition, comparing with the VEGAS GPP estimates (9–12 g C/(m^2·d)), the VPM GPP over maize-growing region was more close to the GPP estimates from in-situ flux sites (12–18 g C/(m^2·d)). Hence, the incorporation of crop-specified module or parameterization can improve the terrestrial ecosystem models to more accurately estimate agricultural productivity and project the climate impact on agroecosystems.

5 Conclusions

The 2012 flash drought in the US Midwest, characterized by high temperature, large cumulative rainfall deficit, and rapid depletion of soil moisture, was the most severe summer drought over the past hundred years. This study used a combined, integrated analysis of flux tower, remote sensing, and modeling analysis, and demonstrated that the large-scale meteorological anomalous patterns in the 2012 growing season significantly affected the US Midwest ecosystems, in particular agroecosystems. This study only investigated the direct and concurrent impacts of flash drought on ecosystems (i.e., phenology, vegetation greenness, and photosynthesis). Ecosystem responses, however, can exceed

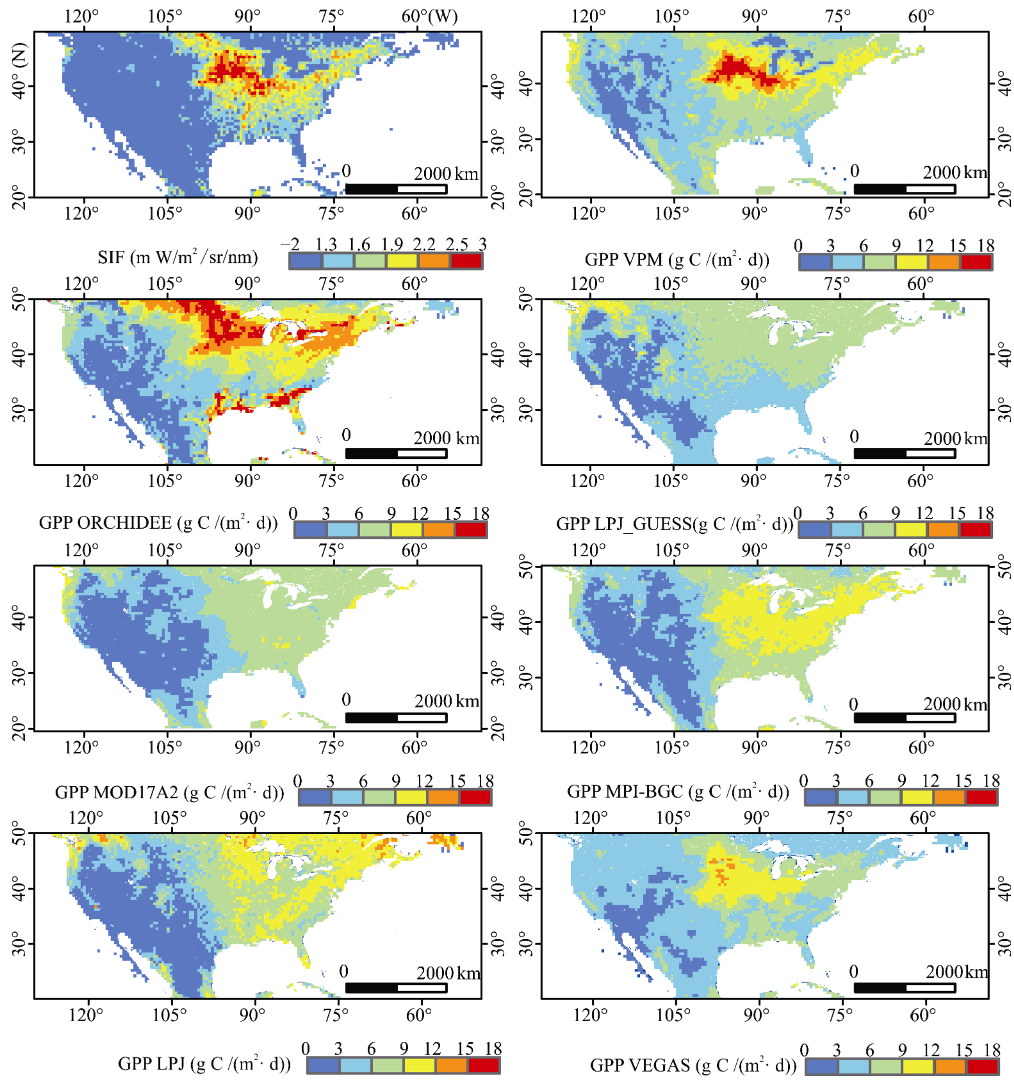

Fig. 8 Comparison of GOME-2 SIF and GPP estimates from the diagnostic models (VPM, MOD17, MPI-BGC), and four process-based DGVMs (ORCHIDEE, JPL_GUESS, JPL, and VEGAS) as part of TRENDY project (http://dgvm.ceh.ac.uk/node/21) in July, 2010

the duration of climate extremes through the time-lagged effects. Thus, the underlying mechanisms of long-term consequences of flash droughts on ecophysiology and ecosystem dynamics, such as reduced plant growth and increase mortality, the changes in species competition, and the pest and pathogen outbreaks in the years following flash droughts, should be better understood in future studies.

Acknowledgement

We would like to thank the FLUXNET for sharing eddy covariance data, and Ms. Yajun Bao for editing figures and tables.

References

Asner G P, Alencar A, 2010. Drought impacts on the amazon forest: the remote sensing perspective. *New Phytologist*, 187(3): 569–578. doi: 10.1111/j.1469-8137.2010.03310.x

Basara J B, Maybourn J N, Peirano C M et al., 2013. Drought and associated impacts in the great plains of the United States—a review. *International Journal of Geosciences*, 4(6B): 72–81. doi: 10.4236/ijg.2013.46A2009

Bigler C, Gavin D G, Gunning C et al., 2007. Drought induces lagged tree mortality in a subalpine forest in the Rocky Mountains. *Oikos*, 116(12): 1983–1994. doi: 10.1111/j.2007.0030-1299.16034.x

Boryan C, Yang Z W, Mueller R et al., 2011. Monitoring US agriculture: the US Department of Agriculture, National Agricultural Statistics Service, Cropland Data Layer Program.

Geocarto International, 26(5): 341–358. doi: 10.1080/10106049.2011.562309

Boyer J S, Byrne P, Cassman K G et al., 2013. The U.S. drought of 2012 in perspective: a call to action. *Global Food Security*, 2(3): 139–143. doi: 10.1016/j.gfs.2013.08.002

Breshears D D, Cobb N S, Rich P M et al., 2005. Regional vegetation die-off in response to global-change-type drought. *Proceedings of the National Academy of Sciences of the United States of America*, 102(42): 15144–15148. doi: 10.1073/pnas.0505734102

Chen T, van der Werf G R, Gobron N et al., 2014. Global cropland monthly gross primary production in the year 2000. *Biogeosciences*, 11(14): 3871–3880. doi: 10.5194/bg-11-3871-2014

Ciais P, Reichstein M, Viovy N et al., 2005. Europe-wide reduction in primary productivity caused by the heat and drought in 2003. *Nature*, 437(7058): 529–533. doi: 10.1038/nature03972

Cook B I, Ault T R, Smerdon J E, 2015. Unprecedented 21st century drought risk in the American Southwest and central plains. *Science Advances*, 1(1): e1400082. doi: 10.1126/sciadv.1400082

Dai A G, 2011. Drought under global warming: a review. *Wiley Interdisciplinary Reviews-Climate Change*, 2(1): 45–65. doi: 10.1002/wcc.81

Dai A G, 2013. Increasing drought under global warming in observations and models. *Nature Climate Change*, 3(1): 52–58. doi: 10.1038/nclimate1633

Daly C, Taylor G H, Gibson W P et al., 2000. High-quality spatial climate data sets for the United States and beyond. *Transactions of the ASAE*, 43(6): 1957–1962. doi: 10.13031/2013.3101

Dunn A L, Barford C C, Wofsy S C et al., 2007. A long-term record of carbon exchange in a boreal black spruce forest: means, responses to interannual variability, and decadal trends. *Global Change Biology*, 13(3): 577–590. doi: 10.1111/j.1365-2486.2006.01221.x

Farooq M, Wahid A, Kobayashi N et al., 2009. Plant drought stress: effects, mechanisms and management. *Agronomy for Sustainable Development*, 29(1): 185–212. doi: 10.1051/agro:2008021

Frank D, Reichstein M, Bahn M et al., 2015. Effects of climate extremes on the terrestrial carbon cycle: concepts, processes and potential future impacts. *Global Change Biology*, 21(8): 2861–2880. doi: 10.1111/gcb.12916

Granier A, Reichstein M, Bréda N et al., 2007. Evidence for soil water control on carbon and water dynamics in European forests during the extremely dry year: 2003. *Agricultural and Forest Meteorology*, 143(1–2): 123–145. doi: 10.1016/j.agrformet.2006.12.004

Guanter L, Zhang Y G, Jung M et al., 2014. Global and time-resolved monitoring of crop photosynthesis with chlorophyll fluorescence. *Proceedings of the National Academy of Sciences of the United States of America*, 111(14): E1327–E1333. doi: 10.1073/pnas.1320008111

Hoerling M, Eischeid J, Kumar A et al., 2014. Causes and predictability of the 2012 great plains drought. *Bulletin of the American Meteorological Society*, 95(2): 269–282. doi: 10.1175/BAMS-D-13-00055.1

Ji L, Peters A J, 2003. Assessing vegetation response to drought in the northern great plains using vegetation and drought indices. *Remote Sensing of Environment*, 87(1): 85–98. doi: 10.1016/S0034-4257(03)00174-3

Jin C, Xiao X M, Wagle P et al., 2015. Effects of in-situ and reanalysis climate data on estimation of cropland gross primary production using the vegetation photosynthesis model. *Agricultural and Forest Meteorology*, 213: 240–250. doi: 10.1016/j.agrformet.2015.07.003

Jin Z N, Ainsworth E A, Leakey A D B et al., 2018. Increasing drought and diminishing benefits of elevated carbon dioxide for soybean yields across the US midwest. *Global Change Biology*, 24(2): e522–e533

Joiner J, Guanter L, Lindstrot R et al., 2013. Global monitoring of terrestrial chlorophyll fluorescence from moderate-spectral-resolution near-infrared satellite measurements: methodology, simulations, and application to GOME-2. *Atmospheric Measurement Techniques*, 6(10): 2803–2823. doi: 10.5194/amt-6-2803-2013

Kellner O, Niyogi D, 2014. Assessing drought vulnerability of agricultural production systems in context of the 2012 drought. *Journal of Animal Science*, 92(7): 2811–2822. doi: 10.2527/jas.2013-7496

Kumar A, Chen M Y, Hoerling M et al., 2013. Do extreme climate events require extreme forcings? *Geophysical Research Letters*, 40(13): 3440–3445. doi: 10.1002/grl.50657

Liu Y, Zhou Y, Ju W et al., 2014. Impacts of droughts on carbon sequestration by China's terrestrial ecosystems from 2000 to 2011. *Biogeosciences*, 11(10): 2583–2599. doi: 10.5194/bg-11-2583-2014

Lobell D B, Roberts M J, Schlenker W et al., 2014. Greater sensitivity to drought accompanies maize yield increase in the U.S. midwest. *Science*, 344(6183): 516–519. doi: 10.1126/science.1251423

Mallya G, Zhao L, Song X C et al., 2013. 2012 midwest drought in the United States. *Journal of Hydrologic Engineering*, 18(7): 737–745. doi: 10.1061/(ASCE)HE.1943-5584.0000786

McKee T B, Doesken N J, Kleist J, 1993. The relationship of drought frequency and duration to time scales. In: *Proceedings of the Eighth Conference on Applied Climatology*. Anaheim, California: AMS, 17–22.

Mesinger F, DiMego G, Kalnay E et al., 2006. North American regional reanalysis. *Bulletin of the American Meteorological Society*, 87(3): 343–360. doi: 10.1175/BAMS-87-3-343

Mo K C, Lettenmaier D P, 2016. Precipitation deficit flash droughts over the United States. *Journal of Hydrometeorology*, 17(4): 1169–1184. doi: 10.1175/JHM-D-15-0158.1

Mueller N D, Butler E E, McKinnon K A et al., 2016. Cooling of US midwest summer temperature extremes from cropland intensification. *Nature Climate Change*, 6(3): 317–322. doi: 10.1038/nclimate2825

Naumann G, Alfieri L, Wyser K et al., 2018. Global changes in drought conditions under different levels of warming. *Geophysical Research Letters*, 45(7): 3285–3296. doi: 10.1002/2017GL076521

Noormets A, Gavazzi M J, Mcnulty S G et al., 2010. Response of carbon fluxes to drought in a coastal plain loblolly pine forest. *Global Change Biology*, 16(1): 272–287. doi: 10.1111/j.1365-2486.2009.01928.x

Otkin J A, Anderson M C, Hain C et al., 2013. Examining rapid onset drought development using the thermal infrared-based evaporative stress index. *Journal of Hydrometeorology*, 14(4): 1057–1074. doi: 10.1175/JHM-D-12-0144.1

Otkin J A, Anderson M C, Hain C et al., 2016. Assessing the evolution of soil moisture and vegetation conditions during the 2012 United States flash drought. *Agricultural and Forest Meteorology*, 218–219: 230–242. doi: 10.1016/j.agrformet.2015.12.065

Otkin J A, Svoboda M, Hunt E D et al., 2018. Flash droughts: a review and assessment of the challenges imposed by rapid-onset droughts in the United States. *Bulletin of the American Meteorological Society*, 99(5): 911–919. doi: 10.1175/BAMS-D-17-0149.1

Phillips O L, van der Heijden G, Lewis S L et al., 2010. Drought-mortality relationships for tropical forests. *New Phytologist*, 187(3): 631–646. doi: 10.1111/j.1469-8137.2010.03359.x

Reddy A R, Chaitanya K V, Vivekanandan M, 2004. Drought-induced responses of photosynthesis and antioxidant metabolism in higher plants. *Journal of Plant Physiology*, 161(11): 1189–1202. doi: 10.1016/j.jplph.2004.01.013

Reichstein M, Ciais P, Papale D et al., 2007. Reduction of ecosystem productivity and respiration during the European summer 2003 climate anomaly: a joint flux tower, remote sensing and modelling analysis. *Global Change Biology*, 13(3): 634–651. doi: 10.1111/j.1365-2486.2006.01224.x

Reyer C P O, Leuzinger S, Rammig A et al., 2013. A plant's perspective of extremes: terrestrial plant responses to changing climatic variability. *Global Change Biology*, 19(1): 75–89. doi: 10.1111/gcb.12023

Schaefer K, Schwalm C R, Williams C et al., 2012. A model-data comparison of gross primary productivity: results from the North American carbon program site synthesis. *Journal of Geophysical Research-Biogeosciences*, 117(G3): G03010. doi: 10.1029/2012JG001960

Schwalm C R, Williams C A, Schaefer K et al., 2010. Assimilation exceeds respiration sensitivity to drought: a FLUXNET synthesis. *Global Change Biology*, 16(2): 657–670. doi: 10.1111/j.1365-2486.2009.01991.x

Schwalm C R, Williams C A, Schaefer K et al., 2012. Reduction in carbon uptake during turn of the century drought in western North America. *Nature Geoscience*, 5(8): 551–556. doi: 10.1038/ngeo1529

Sitch S, Huntingford C, Gedney N et al., 2008. Evaluation of the terrestrial carbon cycle, future plant geography and climate-carbon cycle feedbacks using five Dynamic Global Vegetation Models (DGVMs). *Global Change Biology*, 14(9): 2015–2039. doi: 10.1111/j.1365-2486.2008.01626.x

Svoboda M, LeComte D, Hayes M et al., 2002. The drought monitor. *Bulletin of the American Meteorological Society*, 83(8): 1181–1190. doi: 10.1175/1520-0477-83.8.1181

van der Molen M K, Dolman A J, Ciais P et al., 2011. Drought and ecosystem carbon cycling. *Agricultural and Forest Meteorology*, 151(7): 765–773. doi: 10.1016/j.agrformet.2011.01.018

Vicente-Serrano S M, 2007. Evaluating the impact of drought using remote sensing in a Mediterranean, semi-arid region. *Natural Hazards*, 40(1): 173–208. doi: 10.1007/s11069-006-0009-7

Wehner M, Easterling D R, Lawrimore J H et al., 2011. Projections of future drought in the continental united states and mexico. *Journal of Hydrometeorology*, 12(6): 1359–1377. doi: 10.1175/2011JHM1351.1

Williams I N, Torn M S, Riley W J et al., 2014. Impacts of climate extremes on gross primary production under global warming. *Environmental Research Letters*, 9(9): 101002. doi: 10.1088/1748-9326/9/9/094011

Wolf S, Eugster W, Ammann C et al., 2013. Contrasting response of grassland versus forest carbon and water fluxes to spring drought in Switzerland. *Environmental Research Letters*, 8(3): 089501. doi: 10.1088/1748-9326/8/3/035007

Wuebbles D, Meehl G, Hayhoe K et al., 2014. CMIP5 climate model analyses: climate extremes in the United States. *Bulletin of the American Meteorological Society*, 95(4): 571–583. doi: 10.1175/BAMS-D-12-00172.1

Xiao X M, Hollinger D, Aber J et al., 2004a. Satellite-based modeling of gross primary production in an evergreen needleleaf forest. *Remote Sensing of Environment*, 89(4): 519–534. doi: 10.1016/j.rse.2003.11.008

Xiao X M, Zhang Q Y, Braswell B et al., 2004b. Modeling gross primary production of temperate deciduous broadleaf forest using satellite images and climate data. *Remote Sensing of Environment*, 91(2): 256–270. doi: 10.1016/j.rse.2004.03.010

Xin Q C, Broich M, Suyker A E et al., 2015. Multi-scale evaluation of light use efficiency in MODIS gross primary productivity for croplands in the midwestern United States. *Agricultural and Forest Meteorology*, 201: 111–119. doi: 10.1016/j.agrformet.2014.11.004

Zeng N, Zhao F, Collatz G J et al., 2014. Agricultural green revolution as a driver of increasing atmospheric CO_2 seasonal amplitude. *Nature*, 515(7527): 394–397. doi: 10.1038/nature13893

Zhang L, Xiao J F, Li J et al., 2012. The 2010 spring drought reduced primary productivity in southwestern China. *Environmental Research Letters*, 7(4): 045706. doi: 10.1088/1748-9326/7/4/045706

Zhang Y G, Guanter L, Berry J A et al., 2014. Estimation of vegetation photosynthetic capacity from space-based measurements of chlorophyll fluorescence for terrestrial biosphere models. *Global Change Biology*, 20(12): 3727–3742. doi: 10.1111/gcb.12664

Zhang Y, Xiao X M, Jin C et al., 2016. Consistency between sun-induced chlorophyll fluorescence and gross primary production of vegetation in North America. *Remote Sensing of Environment*, 183: 154–169. doi: 10.1016/j.rse.2016.05.015

Zhang Y Q, Yu Q, Jiang J et al., 2008. Calibration of Terra/MODIS gross primary production over an irrigated cropland on the North China Plain and an alpine meadow on the Tibetan Plateau. *Global Change Biology*, 14(4): 757–767. doi: 10.1111/j.1365-2486.2008.01538.x

Zhao M S, Running S W, 2010. Drought-induced reduction in global terrestrial net primary production from 2000 through 2009. *Science*, 329(5994): 940–943. doi: 10.1126/science.1192666

Zscheischler J, Mahecha M D, von Buttlar J et al., 2014. A few extreme events dominate global interannual variability in gross primary production. *Environmental Research Letters*, 9(3): 035001. doi: 10.1088/1748-9326/9/3/035001

Supplement materials

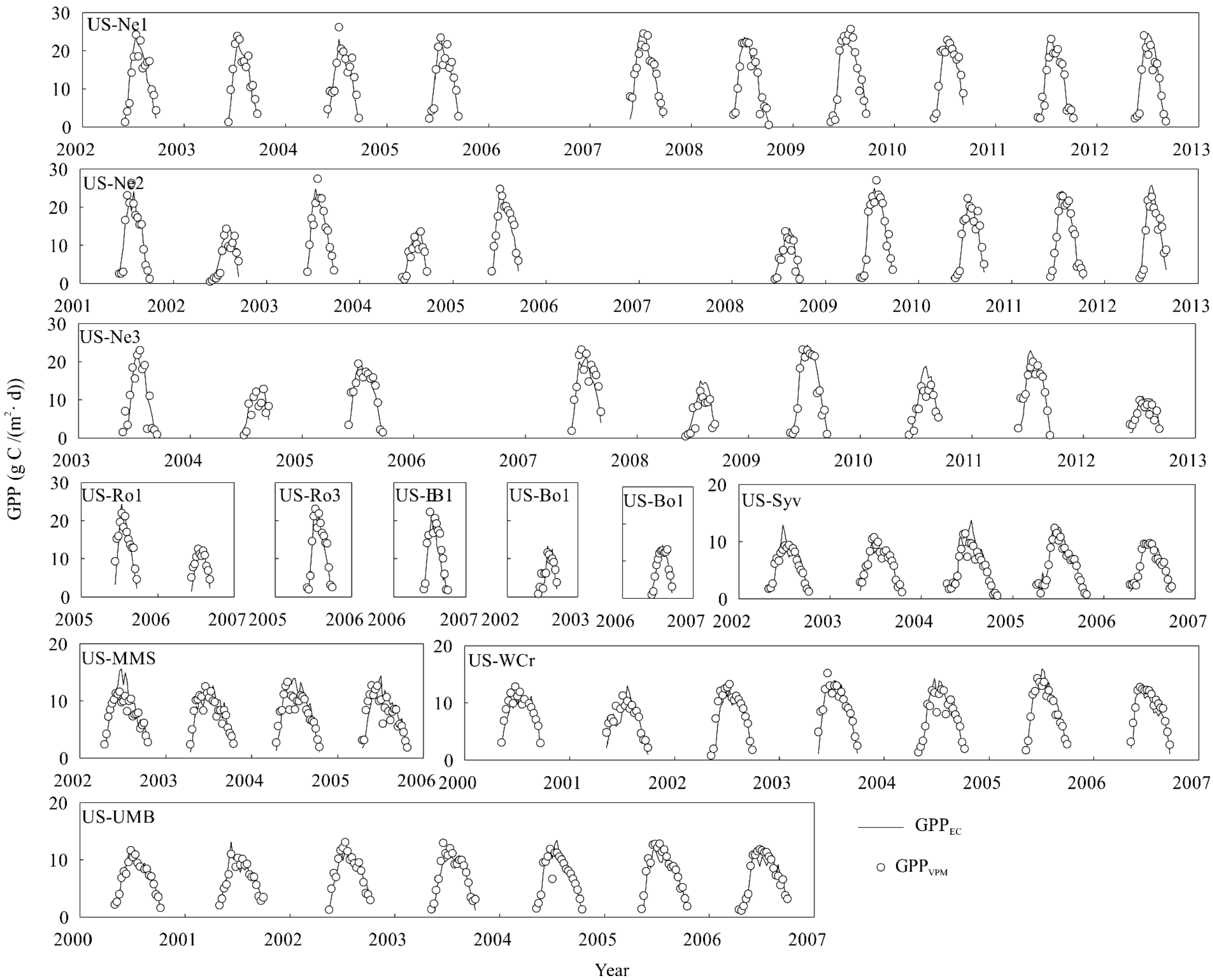

Fig. S1 Seasonal dynamics of 8-day GPP at the AmeriFlux sites in the US Midwest. US-Ne1, US-Ne2, US-Ne3, US-Ro1, US-Ro3, US-IB1, and US-Bo1 are CRO sites for maize and soybean (soybean was highlighted in grey); US-Syv is MF site; US-MMS, US-WCr, and US-UMB are DBF sites. GPP_{EC} is estimated GPP from in-situ eddy tower data; GPP_{VPM} is simulated GPP from the VPM